Proceedings of the 1999 IEEE
International Conference on Robotics & Automation
Detroit, Michigan · May 1999

A Miniature Mobile Parts Feeder: Operating Principles and Simulation Results

Arthur E. Quaid
The Robotics Institute
Carnegie Mellon University
Pittsburgh, Pennsylvania, USA

Abstract

In this work, a miniature mobile vibratory parts feeder is proposed. This feeder, exploiting the unique capabilities of a recently developed closed-loop planar linear motor, is designed to reorient, singulate, and position parts using only horizontal vibrations. The actuators used for generating the feed vibrations are also capable of large planar motions, allowing the feeder to serve multiple overhead robots. This feeder is designed with a minimum of critical physical dimensions, allowing different parts to be fed with only software changes. The basic feed principle is presented, followed by experimental verification. Although a prototype has not yet been fabricated, a model for the motion of parts on the complete feeder is derived and simulation results are presented.

1 Introduction

This work presents the operating principles and simulation results of a novel parts feeder. This feeder is built upon recently developed closed-loop planar linear motor technology [1, 2], and is designed to accept bulk parts, singulate and reorient them, and present them to overhead assembly robots. The main novelty is the feeder's mobility, allowing it to supply multiple overhead robots with parts, even if their workspaces do not overlap. It also has a high degree of programmability and an extremely compact size.

Of course, parts feeding is of critical importance in automated assembly, and has therefore received much attention. Successful commercial bulk feeders include vibratory feeder bowls, the Adept Flexible Parts Feeder [3], and the Sony APOS system [4]. It is interesting to note that all these systems have in common a recirculation path, reorientation facility, and sorting capability. Instead of focusing on each part individually, these feeders provide mechanisms for some of the parts to assume the desired orientations, and allow the rest of the parts to be recirculated. Ensuring the parts are in the proper orientation may be done by mechanical means, such as bowl feeder gates or the Sony APOS tray detents, or through sensing, as in the Adept flex feeder vision system.

Several researchers have explored methods for parts feeding using simple devices. In [5], transverse oscillations of a horizontal plate are used to orient and localize parts by setting up nodes where parts would be attracted. In this manner, parts can be positioned and oriented in the plane using a single actuator and no sensors. In [6], it is shown that horizontal vibrations of a horizontal plate can be used to move parts in the plane. Surprisingly, this technique was extended [7] to independently control the feed directions of multiple parts sitting on the same horizontal plate. The vibration waveform used in [6] will be discussed in more detail below, as the proposed feeder also uses horizontal vibrations.

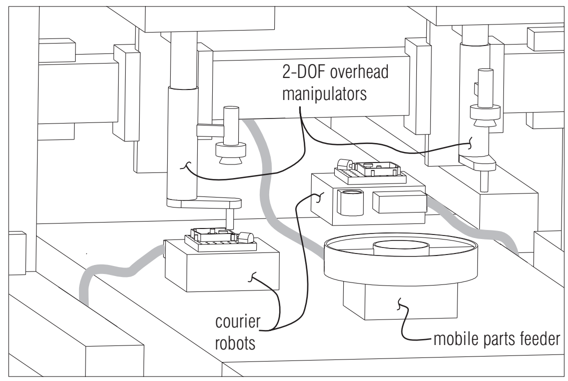

Figure 1: A miniature mobile parts feeder in a minifactory setting: a single feeder supplies parts to multiple low-DOF overhead manipulators.

1.1 Application example

For motivation, an application example will be presented before discussing further details of the feeder. Our particular interest in this feeder is for use in the *minifactory* [8], an automated assembly system that uses small modular robotic components to reduce design, deployment, and changeover times. This system, depicted in Fig. 1, physically consists of a series of tabletop platen tiles connected together to form an extended workspace for courier robots. The courier robots have a novel position sensor [1] integrated into a planar linear motor (Sawyer motor) to enable high-precision closed-loop control. The couriers have a single moving part, ride on air bearings, and can translate large distances along the platen surface (limited only by the length of a tether) and rotate in the plane

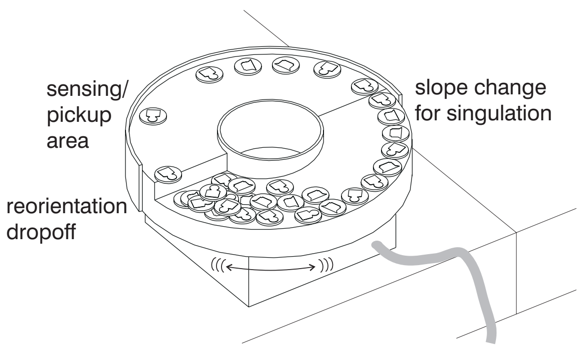

Figure 2: A miniature mobile parts feeder, consisting of a partially sloped annular feed tray (outside edge partially omitted for illustrative purposes) mounted on a planar robot.

by a few degrees. Overhead devices such as simple 2-DOF manipulators, glue dispensers, laser welders, etc. are mounted on fixed bridges above the platens. The couriers move product sub-assemblies from one overhead device to another, cooperating with the overhead devices to perform 4-DOF assembly operations.

The overhead manipulators do not have large workspaces, so parts *must* be fed close to the assembly locations. In this context, it would be very useful to have a mobile parts feeder that can move under the manipulator with an oriented part, allow the manipulator to pick it up, and then move out of the way.

The proposed mobile parts feeder is depicted in Fig. 2. Physically, it consists of a specially shaped feed tray rigidly attached to a planar linear motor. The tray has an annular feed path for parts, with a sloped *ramp* section, and a flat *plateau* section. The motor performs a rotational vibration, resulting in a counter-clockwise motion of the parts. When bulk parts are loaded at the bottom of the ramp, parts slowly climb the ramp, but only near the outside edge, resulting in a single-file line. Once in the plateau section, the parts speed up and spread out. They continue to move around the plateau, where an overhead vision system can be used to identify parts in the correct orientation.[1] Incorrectly oriented parts are reoriented as they pass over the dropoff and return to the pile of bulk parts.

2 Parts feeding principle

In this section, the basic technique for generating part motion is presented. A model is derived and experimental results are presented. As this feeding technique is similar to that used in [6], differences between the approaches are highlighted.

[1] It is also possible to place indentations, fences, etc. in the plateau region to separate parts in the correct orientation without the use of vision. However, unless a removable insert contains all the part specific features, the feeder's flexibility will be compromised.

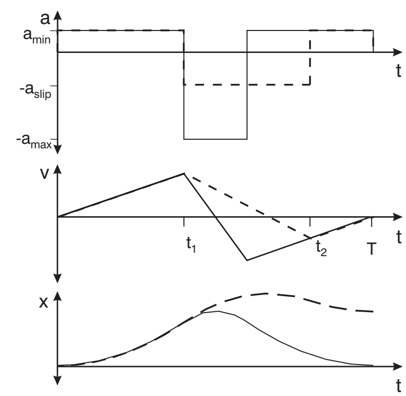

Figure 3: Planar vibratory feeding: at each cycle, the part (dashed trace) moves forward but the tray (solid trace) returns to the original position.

2.1 Parts feeding with a stick-slip waveform

There is a common magician's trick where a tablecloth is removed from under a table setting by quickly jerking the cloth. This trick demonstrates that planar motion can cause relative motion between two objects, and inspired the author's exploration of the application of closed-loop planar linear motors to parts feeding.

Using a smooth plate for the feed tray, motion of parts relative to the tray is achieved by accelerating the feeder rapidly in one direction such that the part slips on the tray, followed by a return to the original position with accelerations slow enough that the part "sticks" to the tray. A periodic waveform with such a *stick-slip* nature is seen in Fig. 3. This waveform is defined as:

$$a(t) = \begin{cases} a_{min} & 0 \le t \le t_1 \\ -a_{max} & t_1 < t \le T - t_1 \\ a_{min} & T - t_1 < t \le T \end{cases} \tag{1}$$

$$v(t) = \begin{cases} a_{min} t & 0 \le t \le t_1 \\ a_{min} t_1 - a_{max}(t - t_1) & t_1 < t \le T - t_1, \\ a_{min}(t - T) & T - t_1 < t \le T \end{cases} \tag{2}$$

where t is the time within the current cycle. The acceleration switch time, t_1 is computed as:

$$t_1 = \frac{a_{max}}{a_{min} + a_{max}} \frac{T}{2}, \tag{3}$$

so that $x(T) - x(0) = \int_0^T v(t) = 0$, and the feeder has no net motion.

The remaining parameters of the waveform to be chosen are the period T, the acceleration during the slip phase a_{max}, and the acceleration during the stick phase a_{min}. The choice of T should keep the waveform frequency low enough to be in the dynamic range of the robot, but high enough to limit the velocities and displacements required of the feeder. For slipping and sticking to occur, a_{max} and a_{min} should be chosen

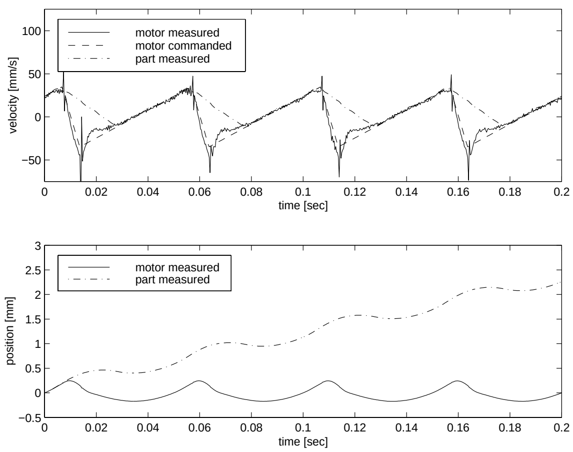

Figure 4: Experimental measurements of feeder and part motion using a stick-slip waveform with $T = 0.05$ s, $a_{min} = 1.6$ m/s^2, $a_{max} = 10.1$ m/s^2. The part is stainless steel and the tray is aluminum; based on the part motion during the slip phase, the coefficient of friction appears to be approximately 0.2.

to meet the constraints $a_{max} > \mu g$ and $a_{min} < \mu g$, where g is the gravitational acceleration and μ is the coefficient of friction between the part and feed tray.

Assuming the part is sticking to the tray at the start of the waveform and its motion is restricted to the direction of tray motion (i.e. no rolling or transverse motion), the part will move as:

$$a_p(t) = \begin{cases} a_{min} & 0 \le t \le t_1 \\ -\mu g & t_1 < t \le t_2 \\ a_{min} & t_2 < t \le T \end{cases} \tag{4}$$

$$v_p(t) = \begin{cases} a_{min} t & 0 \le t \le t_1 \\ a_{min} t_1 - \mu g(t - t_1) & t_1 < t \le t_2 \\ a_{min}(t - T) & t_2 < t \le T. \end{cases} \tag{5}$$

The part catches up to the tray at time

$$t_2 = t_1 + \frac{a_{min} T}{\mu g + a_{min}}, \tag{6}$$

and the average part velocity over one waveform, $\bar{v}_p$, is computed as:

$$\bar{v}_p = \frac{T a_{min}}{2} \left(\frac{-1}{1 + \frac{a_{min}}{\mu g}} + \frac{1}{1 + \frac{a_{min}}{a_{max}}} \right). \tag{7}$$

To verify the feeding principle, the waveform of Eqs. 1 and 2 was used as the input to one axis of a 3-DOF PD controller controlling a planar linear motor. Parts such as coins, rubber grommets, and plastic pieces with varying friction coefficients were placed on a flat feed tray attached to the motor. Although it was possible to find waveforms that would feed the parts well, not all theoretically acceptable waveforms worked. To investigate further, a stainless steel block containing a glass cube corner was used as the 'part,'

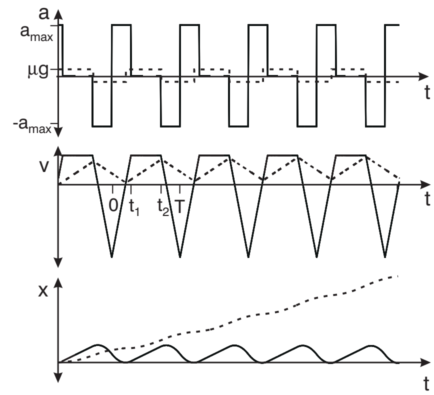

Figure 5: The 'Coulomb pump' waveform can achieve higher part velocities over multiple cycles.

whose position relative to the stationary platen could be measured using a laser interferometer. The motor's position relative to the platen was measured by the integral planar linear motor sensors. Both position measurements were precise and at a high enough bandwidth to allow for velocity measurements by simply taking the difference of consecutive measurements.

Waveforms that worked well appeared as in Fig. 4, with the motor tracking the commanded velocity fairly well. The part velocity deviates from the motor velocity during the slip phase and tracks it closely during the stick phase, as expected. Given the feeder waveform parameters and estimated friction coefficient, $\bar{v}_p$ is computed using Eq. 7 as 11.8 mm/s. In the experiment, the part travelled about 2.48 mm over 0.2 s, for an average velocity of 12.4 mm/s, in close agreement with the computed value.

In waveforms that did not work well, the motor velocity had large deviations from the commanded velocity. Ongoing work includes improved calibration of the motor sensors and actuators, as well as development of controllers with improved tracking abilities.

2.2 Parts feeding with a Coulomb pump waveform

In [6, 7] a *Coulomb pump* waveform is used to achieve part motion in the plane. The waveforms are given in [6] by:

$$a_t(t) = \begin{cases} a_{max} & 0 \le t < t_1 \\ 0 & t_1 \le t < t_2 \\ -a_{max} & t_2 \le t < T \end{cases} \tag{8}$$

$$v_t(t) = \begin{cases} a_{max}\left[\frac{T}{4}(z^2 - 1) + t\right] & 0 \le t < t_1 \\ a_{max}\frac{T}{4}(z - 1)^2 & t_1 \le t < t_2 \\ a_{max}\left[\frac{T}{4}(z^2 + 3) - t\right] & t_2 \le t < T, \end{cases} \tag{9}$$

where $t_1 = (1 - z)T/2$, $t_2 = (1 + z)T/2$, and z is a parameter controlling the fraction of a cycle used by the constant velocity portion of the waveform.

As shown in Fig. 5, the part motion changes from cycle to cycle, with each cycle "pumping up" the velocity via the Coulomb friction forces. The part velocity

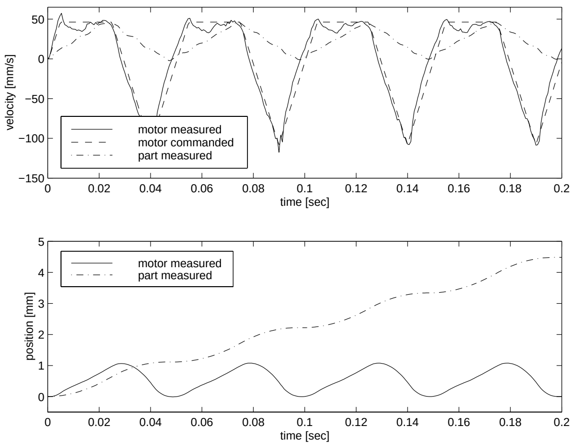

Figure 6: Experimental measurements of feeder and part motion using a Coulomb pump waveform with $T = 0.05$ s, $a_{max} = 10.3$ m/s^2, and $z = 0.37$.

is now best characterized by the *equilibrium velocity*, which is the value that the average waveform velocity eventually reaches, given by [6]:

$$v_{eq} = a_{max} T \frac{z^2}{4}. \tag{10}$$

The Coulomb pump waveform was also implemented on one axis of the planar linear motor. Once again, the main problem was in finding a waveform that the motor followed reasonably well. One example is shown in Fig. 6. Applying Eq. 10, the computed equilibrium velocity is 17.6 mm/s, while the observed velocity in Fig. 6 is 4.5 mm/0.2 s, or 22.5 mm/s, a fairly close match.

The examples shown in Fig. 4 and Fig. 6 (which both use the same part and similar waveform frequencies and maximum accelerations) show that the Coulomb pump waveform has a higher part velocity than the stick-slip waveform, but requires larger velocity and translations from the feeder. The larger forward accelerations of this waveform also appear to cause problems for sloped feed trays, as mentioned later in the Sec. 3.2.

3 A miniature mobile parts feeder

Given the ability to produce part motions using the waveforms discussed above, how can this capability be used for singulating and reorienting bulk parts?

First, if the feed tray (rigidly attached to the planar linear motor) provides a loop for the parts to travel around, the type of recirculation path found in successful commercial parts feeders can be duplicated very compactly within the feed tray. The particular loop chosen is that of an annulus, so that a single rotational vibration waveform of the feeder will suffice to keep the parts flowing around the loop.

Parts must be singulated both radially and along

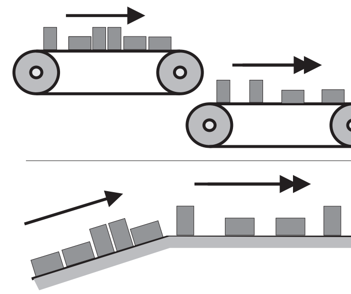

Figure 7: A change of feed velocity based on part position can singulate parts in the direction of motion. This technique can be implemented with conveyors (above) or a sloped feed tray (below).

the circumferential feed path. Along the direction of feeding, if the feed rate increases as a function of position, the parts will tend to spread out. This technique is used in the dual conveyors of the Adept Flexible Parts Feeder [3], schematically shown in the top half of Fig. 7, where one conveyor drops parts onto a faster conveyor. To achieve a similar effect for the proposed feeder, a sloped section may be added to the feeder tray. Assuming that parts will climb up the ramp, but at a slower rate than if they were on a flat surface, the parts on the flat plateau region at the top of the ramp will be singulated in the direction of motion relative to the parts on the ramp section, as depicted in the bottom half of Fig. 7. Simulation results in the next section support this conclusion.

Two effects were expected to provide singulation radially across the feed path. First, the parts were expected to move locally along tangents, which would tend to make them collect towards the outer wall of the feed tray. In addition, the ramp section does not have a constant slope, but gets steeper with decreasing radius. If the waveform is selected carefully, it could be possible to cause parts to slide back down the ramp for small radii, but still climb at larger radii. This technique would allow for a variable-width feeding region at the outer wall of the feed tray. Simulation results below examine these effects.

Once singulated and in the plateau region, an overhead vision system can be used to detect parts in the correct orientation, similar to the Adept flex feeder. The feeder can then move[2] to deliver the parts to an overhead manipulator for assembly.

Incorrectly oriented parts rejected by the vision system continue around the feed path and pass over the dropoff (a nice side-effect of the ramp section), which allows for a reorientation. This effect allows for reorienting parts out of the plane, despite a feeder that is restricted to planar motions. Depending on the part materials, part size and shape, and dropoff height, the part might always just flip over or might assume a more random orientation change. This aspect of the

[2]Of course, it must move with small enough accelerations that the parts don't slide relative to the feed tray.

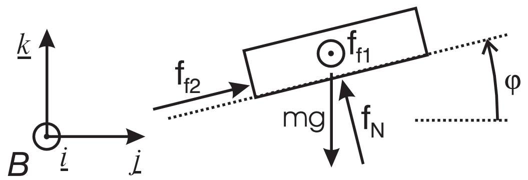

Figure 8: Local free body diagram for a part on an annular tray. (⊙ denotes a vector pointing out of the page.)

feeder is not investigated further in this work.

Although the proposed feeder physically resembles a vibratory bowl feeder, it is important to note the major differences. First, the proposed feeder design is intended for use where feeder bowls custom-designed for parts would be impractical because of re-use requirements or long lead times, and where required feed rates are modest. Conceptually, the feeder operation actually resembles the Adept flexible feeder (with the ramp singulation replacing the double conveyors and both using vision for parts selection) more than a bowl feeder. Second, the use of planar linear motor technology for generation of vibrations allows the feeder to be compact and mobile, permitting it to deliver parts directly to the assembly location, which is especially important for the minifactory application.

3.1 Dynamic model

In this section, a dynamic model is derived for a part on the feed tray discussed in the previous section. The part is assumed to be a point mass that stays in contact with the feed tray, and a Coulomb friction model is assumed. A free-body diagram of the part on the ramped section of the tray is shown in Fig. 8. Coordinate frame B is an inertial (not accelerating) reference frame aligned with the part *at this particular instant in time*.[3] The dynamics of both a sticking case and slipping case must be considered. The dynamics problem is to determine the acceleration of the part along the tray given the part and tray positions and velocities.

By inspection of the free-body diagram, the part dynamics are given by:

$$\begin{aligned} \ddot{x} &= f_{f1}/m & (11)\\ \ddot{y} &= f_{f2}\cos(\varphi)/m - f_N sin(\varphi)/m & (12)\\ \ddot{z} &= f_{f2}\sin(\varphi)/m + f_N cos(\varphi)/m - g, & (13) \end{aligned}$$

where $f_{f1,2}$, f_N, g, and φ are defined in Fig. 8.

For the slipping case, Coulomb's law gives:

$$\mathbf{f}_f = \begin{bmatrix} f_{f1} \\ f_{f2}\cos(\varphi) \\ f_{f2}\sin(\varphi) \end{bmatrix} = \mu f_N \frac{\mathbf{v}_p - \mathbf{v}_t}{\|\mathbf{v}_p - \mathbf{v}_t\|}, \qquad (14)$$

where $\mathbf{v}_p$ is the part velocity, and $\mathbf{v}_t$ is the local tray velocity, both expressed in coordinate frame B.

[3] In the simulation, each time step uses a different frame B.

Assuming the part stays on the surface of the feed tray, there is an additional kinematic constraint on the part acceleration [9]:

$$\ddot{z} = \tan(\varphi)(\ddot{y} - 2\dot{r}\dot{\theta} - r\ddot{\theta}_t), \qquad (15)$$

where r and θ give the part position in polar coordinates relative to the center of the feeder, and θ_t is the rotation angle of the feeder.

To solve for f_N, Eqs. 12 and 13 are substituted into Eq. 15, giving after simplification:

$$f_N = mg\cos(\varphi) - 2m\sin(\varphi)\dot{r}\dot{\theta} - m\ddot{\theta}_t\sin(\varphi). \qquad (16)$$

This result for f_N can then be substituted into Eq. 14 to get $f_{f1,2}$, and Eqs. 11-13 to compute the part acceleration for the slipping case at a given instant in time. Because coordinate frame B is only valid at an instant in time, the acceleration vector must be transformed to a coordinate frame fixed to the workspace before integration.

For the sticking case, the part is fixed relative to the feed tray, and the part accelerations are given based on the tray motion and part position:

$$\begin{aligned} \ddot{x} &= -r\dot{\theta}_t^2 & (17)\\ \ddot{y} &= r\ddot{\theta}_t & (18)\\ \ddot{z} &= 0, & (19) \end{aligned}$$

To check whether the friction forces are sufficient to keep the part stuck to the feed tray, these acceleration values are substituted into Eqs. 11-13, which can be solved for f_N and $f_{f1,2}$:

$$\begin{aligned} f_N &= -mr\ddot{\theta}_t\sin(\varphi) + mg\cos(\varphi) & (20)\\ f_{f1} &= -mr\dot{\theta}_t^2 & (21)\\ f_{f2} &= mr\ddot{\theta}_t\cos(\varphi) - mg\sin(\varphi). & (22) \end{aligned}$$

Both the sticking and sliding equations are evaluated every simulation iteration. The sticking mode results are used if $\|[f_{f1}\ f_{f2}]^T\| < \mu f_N$ (which indicates that the friction forces are sufficient to maintain sticking), and the relative velocity $\|\mathbf{v}_p - \mathbf{v}_t\|$ is below some threshold. Otherwise, the sliding mode results are used. For both cases, the sign of f_N is checked to be sure the part does not leave the tray surface.

3.2 Simulation results

In this section, simulation results are presented for a feeder with an outer radius of 90 mm, an inner radius of 30 mm, and a 180° ramp with a total height change of 20 mm. The part mass is chosen as 20 g, with a coefficient of friction between the part and tray of $\mu = 0.2$. The tray is set to follow a rotational stick-slip waveform, with parameters $T = 1/30$ s, $a_{min} = 9.0\mu g$ rad/s^2, and $a_{max} = 66.7\mu g$ rad/s^2. The initial position of the part is set to a polar array of positions on the tray, with zero initial velocity. For each starting position, the part motion is simulated for 5 s, and the

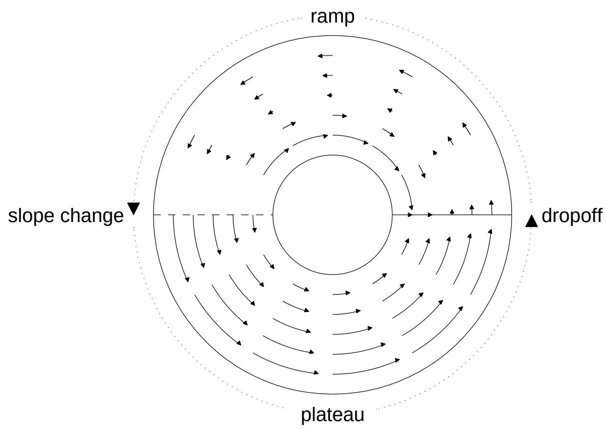

Figure 9: Simulation results show parts climbing the curved ramp, and singulation occurring in the radial and circumferential directions.

sequence of part positions was recorded.

Results for each part starting position are shown in Fig. 9. Note that parts only feed up the ramp if they are close to the outer radius of the feeder, which should cause the parts to form a single-file line, singulating them in the radial direction. The part velocity on the plateau section is much faster than that on the ramp, suggesting that singulation along the direction of motion should also work well. It is surprising that the parts move along nearly perfect arcs, instead of veering off in more of a tangent direction. This effect can be understood by noting that the parts move in a series of small incremental steps that closely approximate a circle. Also, sticking resets the radial velocity of the part to zero every cycle. A depiction of the parts flow in the feeder loosely based on the these simulation results is shown in Fig. 2.

A simulation of the feeder using the Coulomb pump waveform was also attempted. However, it was difficult to get the parts to climb the ramp except for very gradual slopes, with 5 mm or less rise over the 180° ramp. The reason for this difficulty appears to be related to the higher forward acceleration of the tray, which makes the average part velocity highly sensitive to the ramp angle [9].

4 Discussion

The design, operation, and simulation of a novel miniature mobile parts feeder was presented. Experimental results of the basic feed principle confirmed the feed model. Simulation results indicate a promising ability to feed and singulate parts within a compact recirculating device.

Open problems include choosing the waveform parameters given a particular feed tray and part, and designing a feed tray for a family of parts given the limitations of the planar linear motor actuators. In addition, waveforms other than the stick-slip or Coulomb pump can be considered. A hybrid waveform that combines their advantages or the formulation an optimal waveform would improve performance.

There are a number of potential limitations of this feeder. Parts must be stable enough in their pickup orientation to survive the trip up the ramp and the vibrations without falling over. Parts that tend to nest will probably not be singulated properly. Parts may become stuck on the transition between the ramp and plateau, even if it is rounded. Feed rates may be too slow to be useful in a real automated assembly system. However, the results so far are encouraging enough that we intend to build a prototype parts feeder of this type. Fabrication techniques for the feed tray are being considered, and improved calibration and control of the planar linear motor to allow for more precise tracking of the commanded waveforms is being investigated.

Acknowledgements

The author wishes to thank Matt Mason for helpful discussions and especially for suggesting the use of ramps for singulation purposes, and Ralph Hollis and other MSL members for encouragement and support. This work is supported in part by NSF grants DMI-9523156 and CDA-9503992. The author is supported by an AT&T Foundation Fellowship.

References

[1] Z. J. Butler, A. A. Rizzi, and R. L. Hollis, "Integrated precision 3-DOF position sensor for planar linear motors," in *Proc. IEEE Int'l Conf. on Robotics and Automation*, pp. 3109–3114, May 1998.

[2] A. E. Quaid and R. L. Hollis, "3-DOF closed-loop control for planar linear motors," in *Proc. IEEE Int'l Conf. on Robotics and Automation*, pp. 2488–2493, May 1998.

[3] D. Gudmundsson and K. Goldberg, "Tuning robotic part feeder parameters to maximize throughput," in *Proc. IEEE Int'l Conf. on Robotics and Automation*, pp. 2440–2445, April 1997.

[4] J. Krishnaswamy, M. J. Jakiela, and D. E. Whitney, "Mechanics of vibration-assisted entrapment with application to design," in *Proc. IEEE Int'l Conf. on Robotics and Automation*, pp. 838–845, April 1996.

[5] K.-F. Böhringer, V. Bhatt, and K. Y. Goldberg, "Sensorless manipulation using transverse vibrations of a plate," in *Proc. IEEE Int'l Conf. on Robotics and Automation*, pp. 1989–1996, May 1995.

[6] D. Reznik and J. Canny, "The Coulomb pump: a novel parts feeding method using a horizontally-vibrating surface," in *Proc. Int'l Conf. on Intelligent Robots and Systems*, pp. 869–874, 1998.

[7] D. Reznik and J. Canny, "A flat rigid plate is a universal planar manipulator," in *Proc. Int'l Conf. on Intelligent Robots and Systems*, pp. 1471–1477, 1998.

[8] A. A. Rizzi, J. Gowdy, and R. L. Hollis, "Agile assembly architecture: an agent based approach to modular precision assembly systems," in *Proc. IEEE Int'l Conf. on Robotics and Automation*, pp. 1511–1516, April 1997.

[9] A. E. Quaid, "A miniature mobile parts feeder: Operating principles and simulation results," Tech. Rep. CMU-RI-TR-98-26, The Robotics Institute, Carnegie Mellon University, 1998.